

Anders Halldin
 Yohei Jinno
 Silvia Galli
 Mats Ander
 Magnus Jacobsson
 Ryo Jimbo

Implant stability and bone remodeling up to 84 days of implantation with an initial static strain. An *in vivo* and theoretical investigation

Authors' affiliations:

Anders Halldin, Yohei Jinno, Silvia Galli, Magnus Jacobsson, Ryo Jimbo, Department of Prosthodontics, Faculty of Odontology, Malmö University, Malmö, Sweden
 Anders Halldin, DENTSPLY Implants, Mölndal, Sweden
 Mats Ander, Department of Applied Mechanics, Chalmers University of Technology, Göteborg, Sweden

Corresponding author:

Anders Halldin
 Department of Prosthodontics, Faculty of Odontology, Malmö University, 205 06 Malmö, Sweden
 Tel.: +46 40 665 70 00
 Fax: +46 40 92 53 59
 e-mail: anders.halldin@mah.se

Key words: bone condensation, implant stability, *in vivo*, remodeling, static strain

Abstract

Objectives: When implants are inserted, the initial implant stability is dependent on the mechanical stability. To increase the initial stability, it was hypothesized that bone condensation implants will enhance the mechanical stability initially and that the moderately rough surface will further contribute to the secondary stability by enhanced osseointegration. It was further hypothesized that as the healing progresses the difference in removal torque will diminish. In addition, a 3D model was developed to simulate the interfacial shear strength. This was converted to a theoretical removal torque that was compared to the removal torque obtained *in vivo*.

Material and methods: Condensation implants, inducing bone strains of 0.015, were installed into the left tibia of 24 rabbits. Non-condensation implants were installed into the right tibia. All implants had a moderately rough surface. The implants had an implantation time of 7, 28, or 84 days before the removal torque was measured. The interfacial shear strength at different healing time was estimated by the means of finite element method.

Results: At 7 days of healing, the condensation implant had an increased removal torque compared to the non-bone-condensation implant. At 28 and 84 days of healing, there was no difference in removal torque. The simulated interfacial shear strength ratios of bone condensation implants at different implantation time were in line with the *in vivo* data.

Conclusions: Moderately rough implants that initially induce bone strain during installation have increased stability during the early healing period. In addition, the finite element method may be used to evaluate differences in interlocking capacity.

Subsequent to implant placement, the healing process is initiated which eventually leads to formation of new bone immediately adjacent to the implant surface. Directly after implant installation, the implant stability depends solely on the mechanical contact between the surrounding bone (old bone) and the implant. During successful healing new bone formation enhances the implant stability over time (Cochran 2006; Coelho & Jimbo 2014). The degree of initial implant stability (degree of resistance to micromotion) is affected by the implant macrodesign and its relation to the osteotomy preparation. Micromotion of the implant gives rise to interfacial tissue deformations (i.e. strain) that in turn, affect the type of tissue that is formed (Morgan & Einhorn 2013; Coelho et al. 2015). Thus, it is important that sufficient implant stability is obtained to achieve osseointegration. Szmukler-Moncler et al. (1998) sug-

gested that the micro motions should be below 50–150 μm to avoid fibrous tissue encapsulation of the implant. Several theories have been developed to explain the mechanisms that control bone morphogenesis and tissue generation that is based on interfragmentary strain (Pauwels 1960; Perren & Cordey 1980; Carter et al. 1998). Perren & Cordey (1980) suggested that strain levels of less than 0.02 is a prerequisite for bone formation while Carter et al. (1998) proposed that the type of tissue that is formed depends on the hydrostatic pressure and by the tensile strain history. Naturally the bone-implant interfacial shear strength and implant stability depend on the type of tissue developed. Barewal et al. (2003) measured the implant stability by means of a resonance frequency method for various qualities of bone and reported that implants placed in bone of poor quality presented a decrease in resonance

Date:

Accepted 7 November 2015

To cite this article:

Halldin A, Jinno Y, Galli S, Ander M, Jacobsson M, Jimbo R. Implant stability and bone remodeling up to 84 days of implantation with an initial static strain. An *in vivo* and theoretical investigation. *Clin. Oral Impl. Res.* 27, 2016, 1310–1316
 doi: 10.1111/clr.12748

frequency after 2–3 weeks. It was suggested that this phenomenon could be interpreted as a decrease of the implant stability. A plethora of research has been conducted to reduce the micromotion of the implant by modification of the Implant surface at the micro level in order to promote and enhance osseointegration (Coelho et al. 2015). As of today, the moderately roughened oral implants dominate the market, based on the scientific evidence that these surfaces provide rapid and strong bone response (Albrektsson & Wennerberg 2004; Wennerberg & Albrektsson 2009). A general trend in the *in vivo* experiments is that increased S_a value results in increased interfacial shear strength (Loberg et al. 2010). By use of the finite element method Halldin et al. (2015) estimated the interfacial shear strength for different surface structures. It was found that a surface with a S_a value of 1.51 theoretically had a 45% increased interfacial shear strength at 12 weeks of healing compared to a surface with an S_a value of 0.91. Using linear regression between *in vivo* removal torque and S_a values presented by Loberg et al. (2010) resulted in an increase in removal torque of 48% for a S_a value of 1.51 compared to 0.91. In previously conducted *in vivo* studies by Halldin et al. (2011, 2014b), turned implants that induced bone strains of 0.015 (moderate) presented an increased removal torque at 3, 13, and 24 days compared to implants that did not induced bone strain (Halldin et al. 2011, 2014b). The removal torque for this moderate bone condensation implant decreased over time due to reduced pressure on the surface (Halldin et al. 2014b). The reduced pressure over time was suggested to be caused by an initially dominating viscoelastic relaxation and later dominating bone remodeling (Halldin et al. 2014b). However, the removal torque of the moderate bone condensation implants seems to merge with that of the non-bone-condensation implants at ~30 days of healing (Halldin et al. 2014b). To simulate the viscoelastic relaxation and remodeling behavior, Halldin et al. (2014a) developed a viscoelastic constitutive model. It was shown that with appropriate model parameters, the constitutive model captures the relaxation and remodeling behavior of bone which means that the model can be used to estimate the change of pressure on the implant surface over time. Thus, based on these theoretical findings and the previous studies with turned implants (Halldin et al. 2011, 2014b), It was hypothesized that bone condensation implants will enhance the mechanical stability initially

and that the moderately rough surface will further contribute to the secondary stability by enhanced osseointegration.

Thus, as the healing progresses the difference in implant stability, as measured by removal torque between bone condensation implants and non-bone condensation implants, will diminish. In order to test this hypothesis bone condensation implants and non-bone-condensation implants with a moderately rough surface were inserted in rabbit tibiae. The implant stability over time was compared by the means of removal torque measurement. Furthermore, it was hypothesized that by using the finite element method the interfacial shear strength of a bone condensation implants may be estimated.

Material and methods

Implant design

Specially designed screw-shaped implants of titanium (grade 4) were manufactured with tight tolerances to induce controlled bone strains. The designs of the implants were identical to the implants in the study by Halldin et al. (2014b). The test implants comprised of a condensation portion that had an increased diameter of 0.05 mm compared to the cutting portion. These bone condensation implants induced moderate bone strains of 0.015. The control implants had no diametrical increase. All implants had the same surface as the commercially available OsseoSpeed™ implants (DENTSPLY Implants, Mölndal, Sweden).

Interferometry

To confirm that both implant groups had the same surface topography the implant surfaces were characterized by use of optical light interferometry (MicroXAM; ADE Phase shift Technology, Inc., Tucson, AZ, USA). In brief, six randomly selected implants (three controls and three tests) were selected. Each implant was measured on three thread peaks, three valleys, and three flanks (scan area of $264 \times 200 \mu\text{m}$, vertical measurement range of $100 \mu\text{m}$). Data evaluation was performed with the MountainMaps software (Digital Surf, Besançon, France). Waviness and form were filtered with a $50 \times 50 \mu\text{m}$ Gaussian filter. The surfaces were characterized with the surface roughness parameters S_a (μm), S_{dr} (%), and S_{dis} ($1/\mu\text{m}^2$) (definition of them can be found elsewhere (Stout 2000; Thomas 1999)).

Animal study

Twenty-four mature female New Zealand white rabbits (weight 3–4 kg) were used in

this study. The study was approved by the French MINISTÈRE DE L'ENSEIGNEMENT SUPÉRIEUR ET DE LA RECHERCHE and performed at the École Nationale Vétérinaire d'Alfort (Maisons-Alfort, Val-de-Marne, France, approval number, 00391-01). Prior to surgery, 250 $\mu\text{g}/\text{kg}$ of medetomidine (Domitor®, Zoetis, France), 20 mg/kg ketamine (Imalgène 1000®, Merial, Sanofi, France), and 1 mg/kg of diazepam (Valium®, Roche, France) was injected intramuscularly to provide general anesthesia. Subsequently, analgesics 30 $\mu\text{g}/\text{kg}$, buprenorphine (Buprécare, Animalcare, York, UK) was injected subcutaneously and 0.2 mg/kg meloxicam (Metacam®, Boehringer Ingelheim Vetmedica, Inc., St. Joseph, MO, USA) was injected intramuscularly. Thereafter, incision of the skin was made with a #15 blade and the muscle layers and periosteum were elevated and separated from the bone. Osteotomy was prepared in the proximal tibia by drilling with a sequence of burs, starting from a round bur, 2.8 mm drill and finally with a 3.3 mm drill, corresponding to the core diameter of the implants. The osteotomies were performed under constant irrigation with physiological saline solution. Each rabbit received two test implants in one leg (proximal and distal placement) and two control implants on the contralateral side. The implants were inserted with a rotation speed set to 25 revolutions/min using the W&H implant unit (Elcomed, W&H SA-310, Burmoos, Austria). The installation stopped when the superior thread was flush with the cortical bone surface. After implant insertion, the muscle layers were sutured with a resorbable suture (Vicryl3.0), and the skin with a 4-0 nylon suture (Ethicon, Auneau, France). Post-surgically, a patch of fentanyl (25 $\mu\text{g}/\text{h}$, Duragesic®, Janssen Pharmaceutica, Beerse, Belgium) was applied to each animal for 3 days. An antibiotic (enrofloxacin, 200 mg/l, Baytril®, Bayer Animal Health, Leverkusen, Germany) was administered in the water supply for 5 days. The rabbits were kept in separate cages and were allowed to move and eat freely. At 7, 28, and 84 days after implant placement, eight rabbits at each time point were euthanized with an overdose injection of sodium pentobarbital (Euthasol, Virbac, Fort Worth, TX, USA). Each tibia was dissected and excessive soft and hard tissue around the implant square head was carefully removed.

Removal torque measurement

The bone samples were firmly secured with several individual bone pins and the removal torque of the implants was measured. The removal torque, time, and angle of rotation

were recorded with a calibrated torque measurement device (DR-2112 Lorenz Messtechnik GmbH, Alfdorf, Germany) using a constant rotational speed of 0.03 rpm. The torque device was calibrated in the range 50–2000 Nmm with an accuracy of 1 Nmm. The data were sampled with 100 Hz and thereafter analyzed in MATLAB® software 2013b (Mathworks®Inc., Natick, MA, USA). The data were initially smoothed with a running average over a set of 50 data points and the angle of rotation was set to 0 rad when the torque reached 10 Nmm. The fracture torque [T_f] was identified as the maximum torque.

Theoretical interfacial shear strength

In the present study, the test implant induced a pressure at the threads in the condensation region. The magnitude of pressure at the threads was simulated by a radial displacement of the thread profile of 0.025 mm as described in the 2D-axis symmetric model of Hallidin et al. (2011). The 2D simulations were performed using bilinear mature bone material properties without hardening (Table 1). The reduction in pre-stress over time, due to relaxation and remodeling, of mature bone was simulated by use of the constitutive model, illustrated by the rheological model (Fig. 1), (Hallidin et al. 2014a) with model parameter values according to table 6. In brief: the parameters values obtained for simulation (Hallidin et al. 2014a) of the Crowninshield & Pope (1974) experiment were used but recalibrated to represent rabbit bone. The stiffness of springs 1–3 (Fig. 1a) were adjusted to 5008, 2166 and 776 MPa, respectively, to represent Young’s modulus of mature rabbit cortical bone (7950 MPa) (Isaksson et al. 2010). Hence, by changing the spring stiffness values the viscosity was consequently adjusted to fit the relaxation behavior (Hallidin et al. 2014a). Thereafter, the initial strain was increased to achieve a pressure similar to the theoretical thread pressure, simulated in the 2D finite element method, of the test implant. Finally, the remodeling parameter was set to result in no pressure at 30 days which represents the expected theoretical time point when the initially induced bone strains have vanished (Hallidin et al. 2014b). The theoretical interfacial shear strength of the moderately rough surface was simulated using the finite element model described in Hallidin et al. (2015). In brief, a representative patch of the implant surface was selected and a finite element model was developed according to Fig. 1b. The implant was moved until bone failure occurred which was assumed to repre-

Table 1. Mechanical properties of bone during healing derived from mineralization level during healing bone and the relationship between mineralization level and mechanical properties Hallidin et al. (2014a,b)

Healing time		Young’s modulus E (MPa)	Ultimate strain ϵ_u	Yield strain σ_y (MPa)	Comment
Weeks	Days				
0.57	4	2096	0.1153	28.4	Material properties of healing bone (Hallidin et al. 2015)
1	7	2200	0.1122	29.3	
2	14	2738	0.1004	34.2	
4	28	3161	0.0918	37.5	
4.28	30	3189	0.0914	37.8	
12	84	4005	0.0801	44.3	Young’s modulus of mature rabbit bone (Isaksson et al. 2010) and with the ultimate strain and yield strain (Hallidin et al. 2015)
50	350	7950	0.0506	71.3	

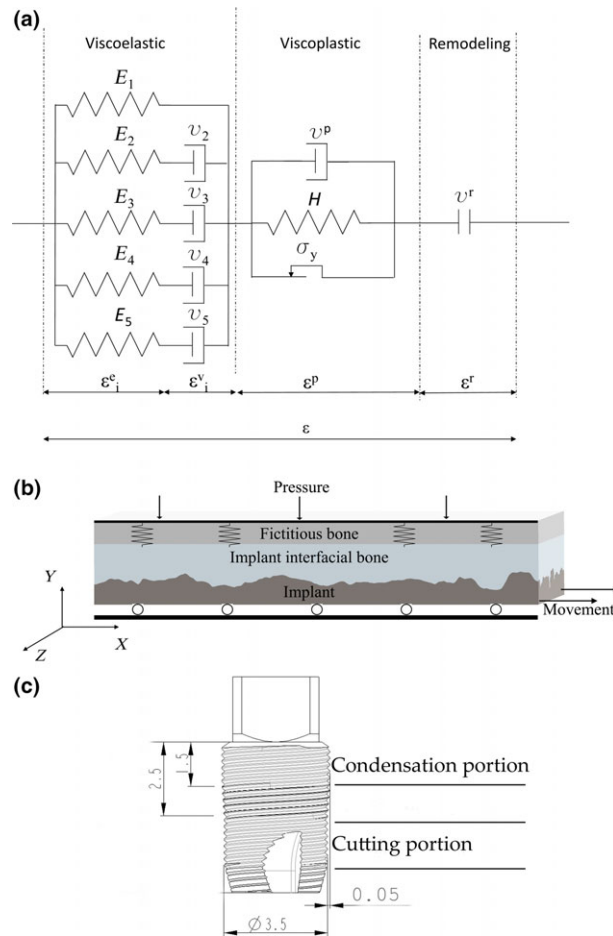


Fig. 1. (a) Rheological model and the model parameters for the constitutive model developed by Hallidin et al. (2014a). (b) FEA Model to simulate the interfacial shear strength of a rough surface exposed to a pressure. (c) Implant design to induce controlled static bone strain.

sent the interfacial shear strength. In the current investigation the interfacial shear strength of a bone condensation implant was simulated with adding an external pressure (Fig. 1b). The pressure was reduced by use of the constitutive model (Hallidin et al. 2014a) to represent relaxation and remodeling material behavior during healing. The control implant was consequently simulated with no pressure (Fig. 1b). In the present study the

theoretical interfacial shear strength was simulated both with mechanical properties of healing bone and mature bone (Hallidin et al. 2014a) (Table 1).

Statistical analysis

Pairwise differences in removal torque measurements between test and control implants that were assumed to be normally distributed were analyzed with Student’s *t*-test. Pairwise

differences in measurements between test and control that were not assumed to be normally distributed were analyzed using Sign Test for Median. Pairwise ratios (test/control) for different healing times were analyzed using Mood Median Test to test the equality of medians from two populations. Interferometry measurements were analyzed using Kruskal–Wallis Test (assumed equal shape). Significance level was set to $P < 0.05$.

Results

Interferometry

There was no difference ($P = 0.287$) in S_a value of test implants (mean $1.55 \mu\text{m}$; std

0.21) compared to control implants (mean $1.49 \mu\text{m}$; std 0.19). There was no difference ($P = 0.441$) in S_{dr} value of test implants (mean 109%; std 44) compared to control (mean 103%; std 49) and no difference ($P = 0.337$) in S_{ds} value of test implants (mean $0.061/\mu\text{m}^2$; std 0.005) compared to control implants (mean $0.061/\mu\text{m}^2$ 0.007). Therefore, the surface structure can be assumed similar.

Animal study

The results of the removal torque measurement (Nmm), for the three different implantation times (7, 28, and 84 days) are presented in a boxplot (Fig. 2a) and Table 2.

One sample (Tibia Proximal 28 days of healing) was unfortunately lost during carefully removing the excessive soft and hard tissue. The corresponding contralateral implant was consequently excluded in the analysis. The ratios between test and control, placed distally, of the present study (at 7, 28, and 84 days).

Theoretical interfacial shear strength

By use of the 2D axisymmetric model a theoretical average normal pressure on the thread profile of 39.5 MPa was obtained. By applying appropriate parameter values the relaxation behavior of mature rabbit bone is captured quite well (Fig. 3a). Using the constitutive

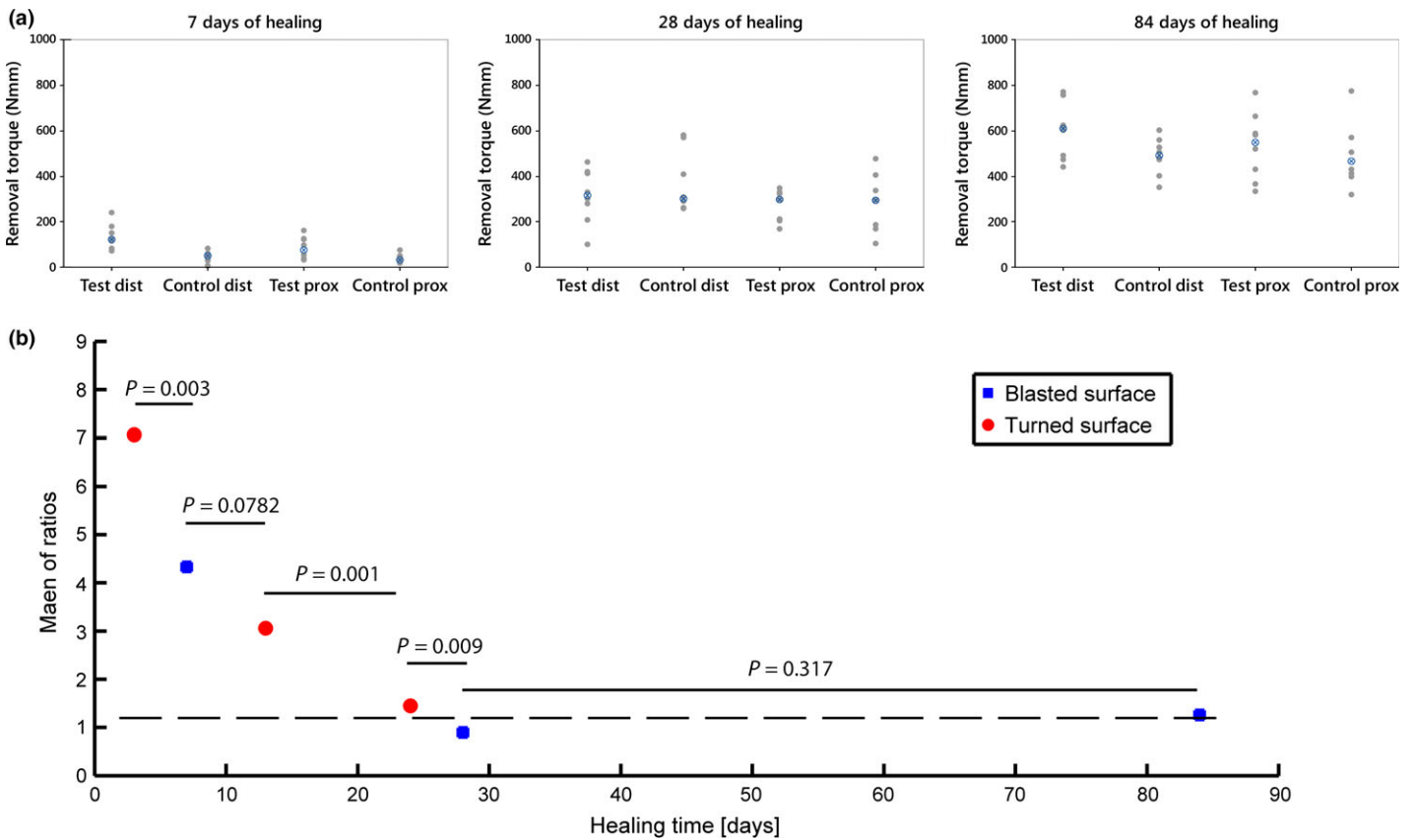


Fig. 2. (a) Individual scatter plots of the removal torque for different implantation times. (b) Removal torque ratios of the present study and the study by Halldin et al. (2011, 2014b). $P < 0.05$ indicates a significant difference in ratios over time.

Table 2. Mean and median of removal torque values and the statistical analysis between the pairwise differences of test and control and the corresponding ratios

Healing time (days)	Site	# Samples	Test		Control		P-value t-Test ¹ Sign test for median ²	Mean pairwise ratio
			Mean torque (SD) Nmm	Median Nmm	Mean torque (SD) Nmm	Median Nmm		
7	Proximal	8	83 (50)	75	39 (18)	32	0.041 ¹	2.3
7	Distal	8	136 (54)	122	47 (23)	50	0.002 ¹	4.3
28	Proximal	7	269 (72)	298	281 (135)	294	0.453 ²	1.2
28	Distal	8	314 (120)	315	371 (134)	300	0.249 ¹	0.9
84	Proximal	8	531 (150)	550	489 (139)	468	0.289 ²	1.1
84	Distal	8	597 (235)	608	488 (80)	492	0.093 ¹	1.3

Subscription is commonly used to differentiate between different statistical methods.

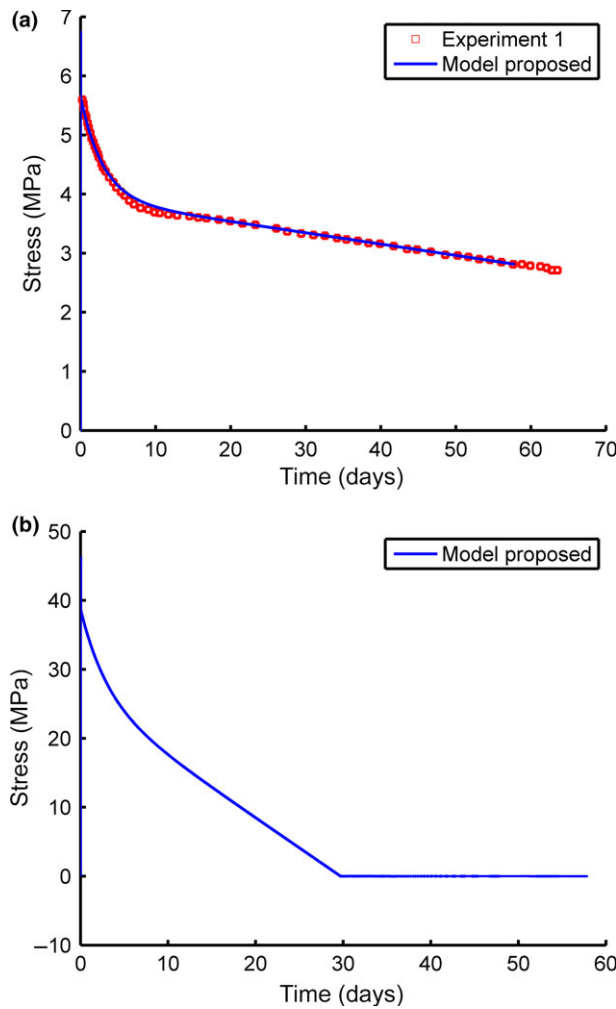


Fig. 3. (a) Simulated behavior of mature bone with calibrated model parameters to fit the relaxation behavior described in Hallidin et al. (2014a). (b) Simulated behavior of increased initial strain to generate a pressure of 39.5 MPa (which represents the theoretical thread pressure of the test implant) and the tuned remodeling parameter value that eliminates the pressure after 30 days.

Table 3. Model parameters used in the constitutive model (Fig. 2) proposed by Hallidin et al. (2014a,b) to simulate the change of pressure over time

Model parameters	Value	Comments
E_1 [MPa]	5009	Represent mature bone Young's modulus of 7950 MPa which was distributed according to ratios found in Hallidin et al. (2014a,b)
E_2 [MPa]	2166	
E_3 [MPa]	775	
E_4 [MPa]	2065	According to the Crowninshield and Pope parameter values obtained in Hallidin et al. (2014a,b)
E_5 [MPa]	11,699	
v_2 [MPa s]	5.55E+08	Calibrated to fit the relaxation behavior in Hallidin et al. (2014a,b) with the Young's modulus of 7950 MPa (fig. 6a)
v_3 [MPa s]	7.48E+04	
v_4 [MPa s]	6.90E+02	According to Crowninshield and Pope parameter values obtained in Hallidin et al. (2014a,b)
v_5 [MPa s]	1.60E-02	
H [MPa]	114	According to Crowninshield and Pope parameter values obtained in Hallidin et al. (2014a,b)
n^p	13.5	
σ_y [MPa]	46.6	
v_p [MPa s]	3.0E+10	
R [s]	2.0E-09	Calibrated to eliminate the initial pressure after 30 days (fig. 6b)

model, with an initial strain to obtain an initial pressure of 39.5 MPa and a tuned remodeling parameter value that eliminated the

pressure after 30 days, the decrease in pressure on the implant surface during healing was simulated (Fig. 3b). The parameter val-

ues used in the constitutive model to simulate the decrease in pressure over time are presented in Table 3. The theoretical interfacial shear strength, with mechanical properties of healing bone together with no pressure over time (represents control implants, simulation C), is presented in Fig. 4a. The theoretical interfacial shear strengths, with mechanical properties of healing bone together with decreased pressure over time (represents test implants, simulation B) and mature bone mechanical properties together with decreased pressure over time (represents test implants, simulation A), are presented in Fig. 4a. The ratios between test and control of the *in vivo* study and the corresponding theoretical ratios are presented in Fig. 4b.

Discussion

An *in vivo* study was conducted to investigate how the implant stability was affected by a moderately rough implant that induced moderate bone strains of 0.015 at the time of implant installation. The implants were allowed to heal in the rabbit tibiae for 7, 28, and 84 days. It was hypothesized that bone condensation implants will enhance the mechanical stability initially and that the moderately rough surface will further contribute to the secondary stability by enhanced osseointegration. The bone condensation implants (i.e. test implants) presented an increased removal torque at 7 days of healing compared to the non-condensation implants (i.e. control implant), whereas at 28 and 84 days of healing no difference in removal torque between bone condensation implants and non-bone condensation implants (Fig. 2b) was observed. In the previous *in vivo* studies by Hallidin et al. (2011, 2014b) turned implants with the same moderate bone condensation level were used. The turned implants had a healing time of 3, 13, and 24 days and the removal torque values were measured with a removal torque device different to that of the one utilized in the current study. In the previous studies, the test (moderate bone condensation) implants presented significantly increased removal torque compared to control implants. The removal torque values of the two different removal torque devices cannot directly be compared. However, if the removal torque ratios (test/control) are calculated respectively for study, they may be compared. Interestingly, there was a similar trend of decreased ratio over time regardless

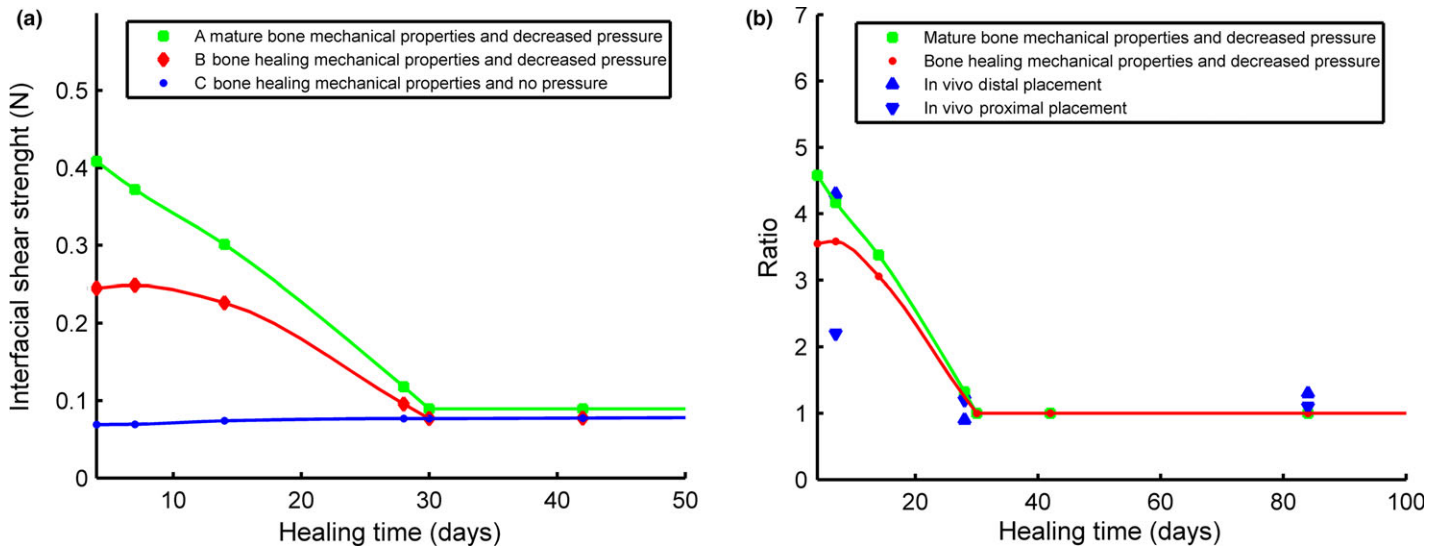


Fig. 4. (a) Simulation of the interfacial shear strength for the test implants with constant mechanical properties of mature bone during healing time and mechanical properties of bone during healing time. Simulation of the interfacial shear strength for the control implants was performed with mechanical properties of bone during healing time. (b) The ratios of the present *in vivo* study and of the simulations.

of the surface micro roughness (turned or moderately roughened) (Fig. 2b). The ratios were considerably higher than 1 (or 100%) during the early healing times, which, in turn, means higher removal torque values for the test implants compared to the control implants. This suggests that the moderate bone condensation implants (test) enhances implant stability during the initial critical phases of healing. When the osseointegration consolidates (at 28 and 84 days) the ratios between test and control tend to reach the value 1 (Fig. 4b). This indicates that the affect moderate bone strains has on implant stability has diminished. It is interesting to observe that the ratio was higher of turned implants at 3 days compared to the ratio of the moderately rough implants at 7 days. This might be related to the fact that the controlled condensation is particularly effective for the retention the first few days of healing (3 days vs. 7 days) regardless of surface structure. The absolute removal torque values of moderately rough surface were increased during healing for both test and control implants, which attests to the favorable bone formation around all implants with a moderately rough surface structure. An interesting reflection from the previous studies of turned implants is that the removal torque decreased over time for the test implants. This might reflect that the decreased pressure, due to relaxation and remodeling, had a more pronounced effect on removal torque than the interlocking of a turned surface structure. In the present study

the removal torque increased over time. Therefore, it might be speculated that the increased interlocking capacity of the moderately rough surface had a more pronounced effect on the removal torque than the reduction in pressure, due to relaxation and remodeling, over time. It should be noted that the removal torque values, especially for the longer healing times, might be affected by bone growth into the cutting feature affecting the results. In addition, the potential grinding effect a structured surface has on the bone might influence the result. The present study used a rabbit model which comprises of a dense cortical bone layer of 3–4 mm and it does not incorporate the implant stability of a potential trabecular bone. The ratios of the present *in vivo* study were compared to the theoretical interfacial shear strength ratios simulated by the use of the 3D finite element model. Interestingly, it was found that the simulated ratios are in line with the *in vivo* ratios. In the 3D simulation the strength of the interfacial bone was increased over time, reflecting healing bone and increased mineralization, that increased the interlocking capacity (Halldin et al. 2015). In the present simulation the interfacial shear strength was simulated both with constant mechanical properties of mature bone and mechanical properties representing healing bone. It may be speculated that mature bone has sporadic contact with the surface structure. Therefore the simulated shear strength of mature bone was assumed to provide the highest interlocking

capacity that can be achieved during healing, thus reflecting only how a decreased pressure affects the interfacial shear strength. In the 3D finite element model the decreased pressure on the surface over time was obtained by use of the constitutive model simulating the relaxation and remodeling behavior of cortical bone (Halldin et al. 2014a). The characteristics of the actual mechanical properties of the *in vivo* bone during healing are unknown. Therefore, the simulation was based on the estimated mechanical properties of the interfacial bone obtained in the study by Halldin et al. (2015). In the present study, the parameters of the constitutive model described in Halldin et al. (2014a) were recalibrated to fit the viscoelastic relaxation and remodeling behavior of rabbit mature bone. It is assumed that when analyzing the ratios these assumptions might have a limited impact. Despite these assumptions, regarding the healing bone mechanical properties and the relaxation and remodeling behavior of rabbit bone (Fig. 3a, b), the simulated ratios had the same trend as the ratios obtained the *in vivo* experiment (Fig. 4b). This implies that finite element analysis, with appropriate material models, may be used to evaluate differences in structural interlocking capacity between two surfaces. In addition, it seems to be a more rapid decrease in ratios during the initial healing which is in line with the findings of Perren et al. (1969) and Cordey et al. (1976). The results of the study suggest that modification of the implant macro geometry in

relationship to the osteotomy preparation, to induce moderate bone strain levels of 0.015 during implant insertion does not result in reduction in stability of moderately rough implants. It is interesting to note that the ratios using finite element method were in line with the *in vivo* ratios. This is an indication that when the condensation level is controlled *in vivo*, the biological outcomes

may be predicted, which could optimize implant design.

Acknowledgement: This work was supported by the Swedish Research Council (621-2010-4760). We would like to acknowledge the assistance of Dr Stig Hansson for the help of removal torque

testing and Mr. Stefan Johnsson at DENTSPLY for preparing all implants.

Conflicts of interests

Mr. Hallidin is employed at DENTSPLY Implants. The other authors have no conflict of interests.

References

- Albrektsson, T. & Wennerberg, A. (2004) Oral implant surfaces: Part 1 – review focusing on topographic and chemical properties of different surfaces and *in vivo* responses to them. *The International journal of prosthodontics* **17**: 536–543.
- Barewal, R.M., Oates, T.W., Meredith, N. & Cochran, D.L. (2003) Resonance frequency measurement of implant stability *in vivo* on implants with a sandblasted and acid-etched surface. *International Journal of Oral and Maxillofacial Implants* **18**: 641–651.
- Carter, D.R., Beaupre, G.S., Giori, N.J. & Helms, J.A. (1998) Mechanobiology of skeletal regeneration. *Clinical Orthopaedics and Related Research*. S41–S55.
- Cochran, D.L. (2006) The evidence for immediate loading of implants. *The Journal of Evidence-Based Dental Practice* **6**: 155–163.
- Coelho, P.G. & Jimbo, R. (2014) Osseointegration of metallic devices: current trends based on implant hardware design. *Archives of Biochemistry and Biophysics* **561**: 99–108.
- Coelho, P.G., Jimbo, R., Tovar, N. & Bonfante, E.A. (2015) Osseointegration: hierarchical designing encompassing the macrometer, micrometer, and nanometer length scales. *Dental Materials* **31**: 37–52.
- Cordey, J., Blumlein, H., Ziegler, W. & Perren, S.M. (1976) Study of the behavior in the course of time of the holding power of cortical screws *in vivo*. *Acta Orthopaedica Belgica* **42**(Suppl. 1): 75–87.
- Crowninshield, R.D. & Pope, M.H. (1974) The response of compact bone in tension at various strain rates. *Annals of Biomedical Engineering* **2**: 217–225.
- Hallidin, A., Ander, M., Jacobsson, M. & Hansson, S. (2014a) On a constitutive material model to capture time dependent behavior of cortical bone. *World Journal of Mechanics* **4**: 348–361.
- Hallidin, A., Ander, M., Jacobsson, M. & Hansson, S. (2015) Simulation of the mechanical interlocking capacity of a rough bone implant surface during healing. *Biomedical Engineering Online* **14**: 45.
- Hallidin, A., Jimbo, R., Johansson, C.B., Wennerberg, A., Jacobsson, M., Albrektsson, T. & Hansson, S. (2011) The effect of static bone strain on implant stability and bone remodeling. *Bone* **49**: 783–789.
- Hallidin, A., Jimbo, R., Johansson, C.B., Wennerberg, A., Jacobsson, M., Albrektsson, T. & Hansson, S. (2014b) Implant stability and bone remodeling after 3 and 13 days of implantation with an initial static strain. *Clinical Implant Dentistry and Related Research* **16**: 383–393.
- Isaksson, H., Harjula, T., Koistinen, A., Iivarinen, J., Seppanen, K., Arokoski, J.P., Brama, P.A., Jurvelin, J.S. & Helminen, H.J. (2010) Collagen and mineral deposition in rabbit cortical bone during maturation and growth: effects on tissue properties. *Journal of Orthopaedic Research* **28**: 1626–1633.
- Loberg, J., Mattisson, I., Hansson, S. & Ahlberg, E. (2010) Characterisation of titanium dental implants I: Critical assessment of surface roughness parameters. *The Open Biomaterials Journal* **2**: 1–8.
- Morgan, E.F. & Einhorn, T.A. (2013) *Biomechanics of Fracture Healing Primer on the Metabolic Bone Diseases and Disorders of Mineral Metabolism*, 8th edn, 99–102. Somerset, NJ, USA: John Wiley & Sons.
- Pauwels, F. (1960) A new theory on the influence of mechanical stimuli on the differentiation of supporting tissue. The tenth contribution to the functional anatomy and causal morphology of the supporting structure. *Zeitschrift für Anatomie und Entwicklungsgeschichte* **121**: 478–515.
- Perren, S.M. & Cordey, J. (1980) The concept of interfragmentary strain. *Current Concepts of Internal Fixation of Fractures*, 63–77. Berlin: Springer-Verlag.
- Perren, S.M., Huggler, A., Russenberger, M., Allgower, M., Mathys, R., Schenk, R., Willenegger, H. & Muller, M.E. (1969) The reaction of cortical bone to compression. *Acta Orthopaedica Scandinavica. Supplementum* **125**: 19–29.
- Stout, K. (2000) *Development of Methods for the Characterisation of Roughness in Three Dimensions*, 216–249. London: Penton Press.
- Szmukler-Moncler, S., Salama, H., Reingewirtz, Y. & Dubruille, J.H. (1998) Timing of loading and effect of micromotion on bone-dental implant interface: review of experimental literature. *Journal of Biomedical Materials Research* **43**: 192–203.
- Thomas, T.R. (1999) *Rough Surfaces*, 133–195. London: Imperial College Press.
- Wennerberg, A. & Albrektsson, T. (2009) Effects of titanium surface topography on bone integration: a systematic review. *Clinical Oral Implants Research* **20**(Suppl. 4): 172–184.